

Light Scattering on Nonspherical Particles: A NAG User Story

T. Rother, J. Wauer, and K. Schmidt
German Aerospace Center
Remote Sensing Technology Institute
D-17235 Neustrelitz

August 18, 2010

1 Introduction

Scattering of electromagnetic waves on nonspherical particles is applicable to remote sensing of the earth's atmosphere as well as in technical and medical diagnostics. Studying the influence of dust like particles on our climate system, estimating size distributions of powder probes, and analyzing red blood cells are only a few examples of where it is used. There are an increasing amount of modern measurement techniques developed during the last decades which make it necessary to take light scattering not only on spheres but on more realistic particles into account. Unfortunately, there are two factors which make this a complex task. Firstly, the numerical effort is much higher than that known for spherical particles within the conventional Mie theory. It depends strongly on the morphology of the particle under consideration and can be performed online only in very specific situations. Secondly, the convergence procedures of the existing approaches are much more complex compared to those used with spheres. To obtain reliable results requires a detailed knowledge of the methodology behind the approach. Otherwise, one can run into a lot of pitfalls.

To overcome these problems we have developed a software package (called *mieschka*) to analyze light scattering on rotationally symmetric particles in fixed and random orientation using an automatic convergence procedure. Moreover, to release practitioners from dealing with those aspects where possible and to provide an easy access to scattering data for use by applications as well as benchmark purposes, we have established a database for spheroidal particles in random orientation. Details of the methodology used can be found in [1].

2 Method and Convergence Procedure

The software package *mieschka* is based on the so-called T-matrix method. With this approach the incident field as well as the scattered field are represented in spherical coordinates by finite series expansions

$$\mathbf{E}^s(k_o\mathbf{r}) = \sum_{\tau=1}^2 \sum_{l=-l_{cut}}^{l_{cut}} \sum_{n=|l|}^{n_{cut}} f_{\tau nl} \Psi_{\tau nl}(k\mathbf{r}) \quad (1)$$

$$\mathbf{E}^{inc}(k\mathbf{r}) = \sum_{\tau=1}^2 \sum_{l=-l_{cut}}^{l_{cut}} \sum_{n=|l|}^{n_{cut}} a_{\tau nl} \text{Rg}\Psi_{\tau nl}(k\mathbf{r}) \quad (2)$$

in terms of appropriate vector expansion functions $\Psi_{\tau nl}(k\mathbf{r})$ and $\text{Rg}\Psi_{\tau nl}(k\mathbf{r})$. The expansion coefficients $f_{\tau nl}$ of the scattered field are calculated from the known coefficients $a_{\tau nl}$ of the incident field by use of the T-matrix relation

$$\mathbf{f} = \mathcal{T} \cdot \mathbf{a} . \quad (3)$$

The T-matrix itself is the product of three matrices,

$$\mathcal{T} = -\mathcal{Q}^{-1} \cdot \text{Rg}\mathcal{Q} . \quad (4)$$

Their elements are boundary integrals over the scatterer surface. Obviously, matrix \mathcal{Q} must be inverted. Thus, the overall convergence of the method depends on the following 4 aspects:

- Accuracy of the calculated boundary integrals
- Accuracy of the matrix inversion
- Number of expansion terms used
- Accuracy of the orientation averaging process used.

The convergence procedures employed are as follows:

2.1 Accuracy of the boundary integrals

The calculation is performed in two steps by use of a 7 point (first step) and a 15 point (second step) Gauss-Kronrod quadrature rule. The width of each integration interval is matched to a pre-determined relative accuracy of integration with respect to these two steps. The actual accuracy of integration achieved as well as the number of the function calls necessary are stored further convergence considerations. The numerical evaluation is realized with the adaptive NAG f90 module *nag_quad_1d*.

2.2 Accuracy of the matrix inversion

To perform the matrix inversion, we have tested several algorithms. Most stable results have been obtained with the two NAG f90 module *nag_gen_lin_sys*. The condition number calculated by these modules is a first check regarding the accuracy of the matrix inversion. The NAG procedures provide a warning that the matrix under consideration has become ill-conditioned. In this case, the user must check the final result obtained very carefully (see also the next procedure).

2.3 Number of terms used in the expansion

Here we have to determine the truncation values n_{cut} of the series expansions (1) and (2). To determine n_{cut} we compare the differential scattering cross-sections in the whole scattering plane for two successive computations (n_{cut} and $n_{cut} + 3$) for light incidence along the axis of symmetry of the particle. The successive computation is stopped if the pre-determined relative accuracy is achieved for 80% of all scattering angles. This procedure has proved to be effective in many applications.

To determine l_{cut} for random orientation an effective phase function is introduced which is calculated from averaging over 9 different angles of orientation. As for n_{cut} , two successive computations (but now with the steps l_{cut} and $l_{cut} + 1$) are performed. The procedure is stopped if the pre-determined relative accuracy is achieved for all scattering angles.

2.4 Accuracy of the orientation averaging process

Two different procedures have been used to perform orientation averaging. One procedure applies numerical integration for orientation averaging, and a second procedure uses an analytical orientation averaging by employing Clebsch-Gordon coefficients. If the numerical integration was used to perform orientation averaging the same procedure as described in the subsection "Accuracy of the boundary integrals" was applied to the phase function at all scattering angles. Due to the rotational symmetry of spheroidal particles this requires now a two-dimensional quadrature rule (procedure *nag_quad_2d* from the NAG f90 library).

In addition, the special function routines of the NAG f90 library have been used to calculate the necessary Bessel and Neumann functions. It should be also emphasized that the detailed error handling and warnings produced by the NAG f90 modules were very helpful especially during the development and validation phase of the *mieschka*.

Fig. 1 shows an intercomparison of the phase functions of a spherical and a spheroidal particle in random orientation. A typical difference in the backscattering region (i.e., for scattering angles larger than 90 degree) can be observed.

3 Database for Spheroidal Scatterers

Very often, we are faced with the situation where the scattering signal from a certain volume element is caused by an ensemble of particles rather than a single particle. Such ensembles of particles are characterized by different geometries, sizes, and dielectric properties. Size averaging then requires a huge amount of scattering calculations which can become a tedious task if nonspherical particles are considered. Having a database with pre-calculated scattering data would therefore be of some benefit for the user. With the above mentioned software package we have established such a data base for spheroidal particles. The geometry of these particles is given by

$$\left(\frac{x}{b}\right)^2 + \left(\frac{y}{b}\right)^2 + \left(\frac{z}{a}\right)^2 = 1 \quad (5)$$

In the data base the geometry is described by the aspect ratio $av = a/b$ (a - semi axis along the axis of symmetry) and the size parameter $kr_{eqv(v)}$ to which the scattering problem can be scaled. An aspect ratio $av > 1$ belongs to prolate spheroids, and $av < 1$ corresponds to oblate ones. The effective radius $r_{eqv(v)} = \sqrt[3]{ab^2}$ represents the radius of the volume equivalent sphere, and k is the wave number of the incident light. For the aspect ratio and the refractive index the following grid was used:

$\Re(n)$	1.31	1.33	1.4	1.5	1.55	1.6	1.7	1.8						
$\Im(n)$	0	0.001	0.005	0.01	0.03	0.05	0.1							
av	0.67	0.714	0.77	0.82	0.87	0.93	1	1.075	1.15	1.22	1.3	1.4	1.5	

The resolution with respect to the size parameter is $\Delta kr_{eqv(v)} = 0.2$. This allows for an interpolation with a sufficient accuracy if intermediate size parameters are needed. This interpolation is realized with certain splines from the NAG fl90 library. The angular resolution in the scattering plane is dependent on the size parameter region:

size parameter	0°-10°	10°-173°	173°-180°
0-20	0.75°	2.5°	0.75°
20-40	0.5°	1.5°	0.5°

Due to these parameters and resolutions the total amount of pre-calculated scattering data sets is nearly 60,000!

Fig. 2 provides an example of the backscattering depolarization of different spheroidal particles. Such charts are of interest in Lidar applications, for example. The bluish regions mark parameter sets with a lower depolarization, while the reddish ones designate larger depolarization values. In general, randomly oriented prolate spheroids ($av > 1$) exhibit larger depolarizations than oblate ones ($av < 1$). In each tile, both regions are clearly separated by the zero-depolarization band originating from spherical particles. It is furthermore seen that, within the chosen parameter range, the largest depolarization differences occur for small real parts and small imaginary parts of the refractive index.

We are currently working on further improvements and enlargements of this data base.

References

- [1] T. Rother: "Electromagnetic Wave Scattering on Nonspherical Particles: Basic Methodology and Simulations", Springer, Berlin Heidelberg New York 2009.

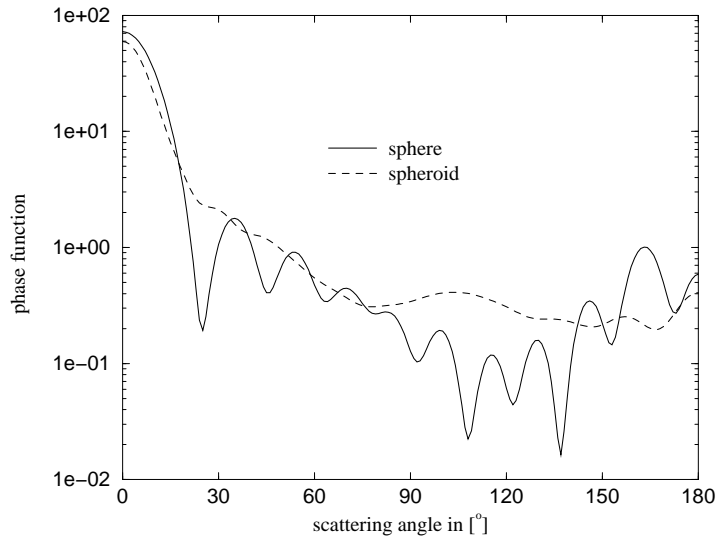


Figure 1: Phase function of a sphere and a prolate spheroid with an aspect ratio of $av=2$. The refractive index of both particles is $n=1.5$. The size parameter of the sphere is $\frac{2\pi r}{\lambda} = 10$. The spheroid has the same volume as the sphere.

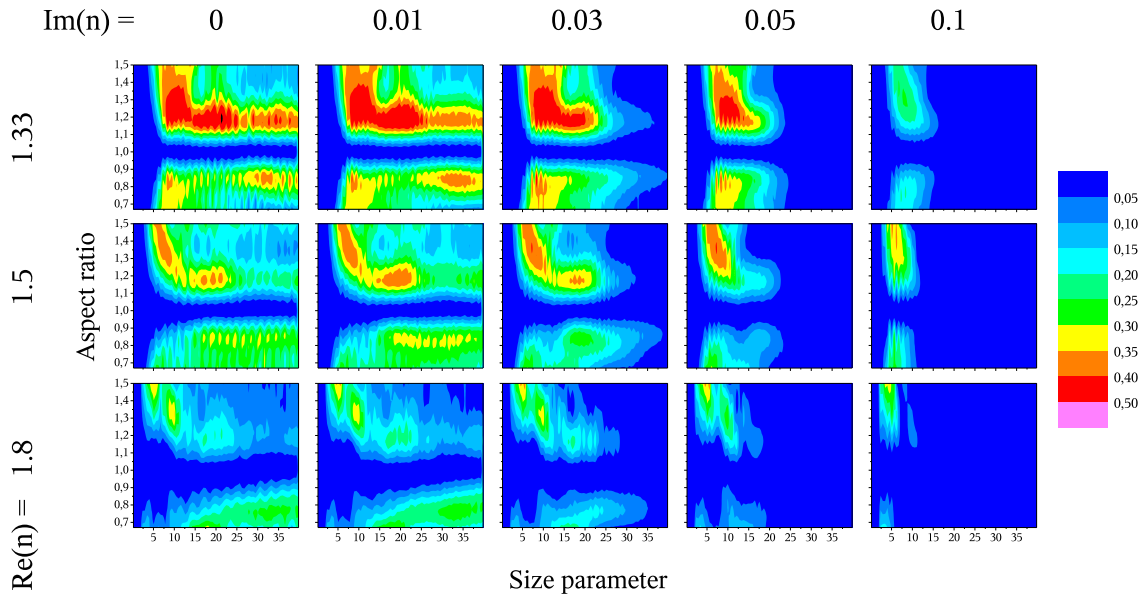


Figure 2: Backscattering depolarization for spheroidal particles in dependence on the refractive index (real and imaginary part), aspect ratio, and size parameter.